Inorganic Chemistry

Article

pubs.acs.org/IC

H-bonded adducts of [2,4,6-{$(C_{10}H_{21}O)_3C_6H_2NH\}_3C_3N_3$] with [$LnM\{PPh_2(C_6H_4CO_2H)\}$] displaying Columnar Mesophases at Room Temperature

Ana B. Miguel-Coello,[†] Manuel Bardají,*[,†] Silverio Coco,*[,†] Bertrand Donnio,[‡,§] Benoît Heinrich,[‡] and Pablo Espinet*[,†]

[†]IU CINQUIMA/Química Inorgánica, Facultad de Ciencias, Universidad de Valladolid, E-47071 Valladolid, Spain

[‡]Institut de Physique et Chimie des Matériaux de Strasbourg (IPCMS), UMR 7504 (CNRS−Université de Strasbourg), 23 rue du Loess, BP 43, 67034 Strasbourg Cedex 2, France

[§]Complex Assemblies of Soft Matter Laboratory (COMPASS), UMI 3254 (CNRS−SOLVAY−University of Pennsylvania), CRTB, 350 George Patterson Boulevard, Bristol, Pennsylvania 19007, United States

Supporting Information

ABSTRACT: Displacement of a labile ligand from appropriate precursor complexes by 2- or 4-$PPh_2C_6H_4COOH$ yields neutral gold(I) and gold(III) [$AuX_n(PPh_2C_6H_4COOH)$] (n = 1, X = Cl; n = 3, X = C_6F_5), cationic gold(I) [$Au(PPh_2C_6H_4COOH)_2$]-(CF_3SO_3), and neutral chromium(0) [$Cr(CO)_5(PPh_2C_6H_4COOH)$] metallo−organic acids. [$AuCl(4\text{-}PPh_2C_6H_4COOH)$], [$Au(C_6F_5)_3(4\text{-}PPh_2C_6H_4COOH)$], and [$Cr(CO)_5(2\text{-}PPh_2C_6H_4COOH)$] have dimeric structures with typical carboxylic H-bond bridges, whereas [$Au(C_6F_5)_3(2\text{-}PPh_2C_6H_4COOH)$] gives a monomeric species with the carboxylic acid H bonded to cocrystallized solvent molecules. All gold-containing acids are emissive at 77 K in the range 404−520 nm and some of them also at 298 K with emission maxima from 441 to 485 nm. Reaction of these acid metal complexes with the triazine mesogen 2,4,6-{$(C_{10}H_{21}O)_3C_6H_2NH\}_3C_3N_3$ affords some new hydrogen-bonded gold(I) and chromium(0) supramolecular adducts, but the related gold(III) complexes do not form adducts. The 4-diphenylphosphinobenzoic adducts display a columnar hexagonal mesophase (Col_{hex}) at room temperature, with a random one-dimensional stacking of the pseudo-discoid triazine−metallo−organic adducts into columns, where the metallo−phosphinoacid fragments act as the fourth branch of the trifold triazine core. The 2-diphenylphosphinobenzoic mixtures do not display mesophases, as they appear in the X-ray studies as mixtures of the triazine and the metallo−phosphinoacid complex. The aggregates are luminescent at 77 K, with emission maxima in the range 419−455 nm.

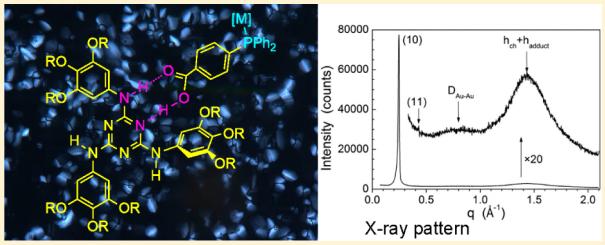

INTRODUCTION

Intermolecular hydrogen bonding can promote molecular self-assembly into ordered supramolecular structures, allowing for engineering of soft materials with specific functionalities.[1] This approach has been used successfully in the construction of organic liquid crystalline architectures. Many examples of simple to highly complex molecular self-assemblies have been reported.[2,3]

There is interest in liquid crystalline systems forming columnar arrangements due to their potential application in opto-electronic devices with some advantageous properties:[4] high charge-carrier mobility along the stacking axis, long-range self-assembling, self-healing and easy processing due to fluidity, solubility in organic solvents, and added properties such as luminescence, conductivity, or magnetism (for metallomesogens).

Metal-containing H-bonded liquid crystals are still rare,[5−11] but smectic and columnar mesophases can be produced by judicious combination of the complementary building blocks. 2,4,6-Triarylamino-1,3,5-triazines equipped by 6 or 9 peripheral alkoxy chains are appropriate bricks to form H-bonded discotic adducts with carboxylic acids and self-organize into liquid crystalline columnar mesophases.[12] We recently extended this concept by integrating metal complexes containing carboxylic acid functions and reported new types of supramolecular metallomesogens, derived from 1:1 association of a triazine and a 4-isocyanobenzoic acid complex of chromium(0), iron(0), molybdenum(0), or tungsten(0). The hexagonal packing into columnar mesophases found for the free triazine was systematically preserved in the metal-containing supramolecular adducts.[13] In contrast, the corresponding gold(I) isocyanobenzoic acid complexes did not produce such adducts, likely because the weakness of the H-bonding interactions with the triazine and the high insolubility of the starting gold complexes makes adduct formation thermodynamically unfavorable. Using the same self-assembly concept, we could prepare mono- and dinuclear thiolatobenzoic gold(I) adducts with the same

Received: May 8, 2014
Published: October 1, 2014

   dx.doi.org/10.1021/ic501039n | *Inorg. Chem.* 2014, 53, 10893−10902

triazine mesogen and demonstrated that the corresponding supramolecular adducts also produce a stable Col_{hex} mesophase at room temperature.[14] In all cases, the supramolecular triazine−metallo−organic acid complexes stack in a complementary manner: the metallic thiolatobenzoic/isocyanobenzoic acid fragment acts as a fourth branch of the triazine core in such a way that the steric crowding is minimized and the interface with the aliphatic continuum is smoothened. In other words, the metal complex moieties are somehow buried into the dominant aliphatic environment in such a way that each discotic unit of adduct appears externally very similar to the free triazine, a disc with aliphatic chains. The versatility of this approach is therefore very promising for the design and construction of room-temperature LC mesophases from metal-containing molecules using other carboxylic acid linkers to connect a metallic fragment to the triazine. A potential consequence of linking additional groups (in this case metal complexes) to a regular discotic molecule is that the new adduct, having a substituent protruding from the central core, is less symmetric, and this descent of symmetry might produce changes in the properties of the material, as studied in less complex systems.[15]

In this study we examine the utility of 2- and 4-diphenylphosphinobenzoic acids (Figure 1). The P atom is a

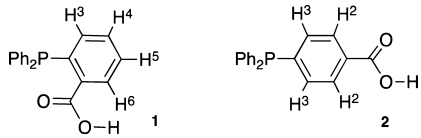

Figure 1. Structures of 2- and 4-diphenylphosphinobenzoic acids and ^{1}H NMR labels.

general donor for any metal fragment, and therefore, these ligands can be used as P ligands in the synthesis of many metal complexes. They have also been used as carboxylate ligands.[16] In line with our previous works on metallo−organic supramolecular assemblies, the carboxylic functional group of these diphenylphosphinobenzoic acids is suitable to produce H bonds. For instance, 2-diphenylphosphinobenzoic acid is a dimer with typical carboxylic acid bridges,[17] and gold(I),[18,19] and copper(I)[20] derivatives have been reported also as H-bonded dimers.

P-containing metallomesogens are uncommon because of the unfavorable tetrahedral geometry imposed by the phosphorus atom.[21] However, we reported recently that the hexagonal columnar architectures produced by aggregation of isocyano− or thiolato−metallo−organic acids to triazines are able to accommodate some structurally voluminous molecular groups between the branches of the triazine, still preserving the mesogenic behavior.[13,14] Achieving the same with phosphine groups as linkers looks more challenging, but in the present study we will show that some liquid crystals can be made. Even more challenging is the use of 2-diphenylphosphinobenzoic acid that, compared with its para isomer, introduces a violent rigid kink in the supramolecule pursued. Three different metal moieties were chosen that provide different features to the potential metallomesogens: linear Au^I, which is expected to be favorable; octahedral $Cr(CO)_5$, which has been shown before to be reasonably favorable and is a good reporter of the bonding interaction through ν(CO) of the carbonyl groups in IR; and square-planar Au^{III}, which has not been checked before. Some of the metal-containing moieties are very demanding sterically and were chosen on purpose to challenge the ability of the triazine to accommodate them into a discotic unit.

RESULTS AND DISCUSSION

Synthesis and Characterization of Diphenylphosphinobenzoic Acid Metal Complexes. Reaction of diphenylphosphinobenzoic acids **1** or **2** with [AuCl(tht)], [Au$(C_6F_5)_3$(tht)], [Au(tht)$_2$]CF_3SO_3 (tht = tetrahydrothiophene), or hexacarbonyl chromium(0) leads to the corresponding gold(I), gold(III), or chromium(0) complexes **3**−**10** (Scheme 1). They are air-stable, white (**3**−**8**) or yellow (**9**−**10**) solids at room temperature and were characterized by CHN analysis, IR, and NMR.

Scheme 1. Synthesis and Molecular Structures of the Gold or Chromium−Organic Acids 3−10[a]

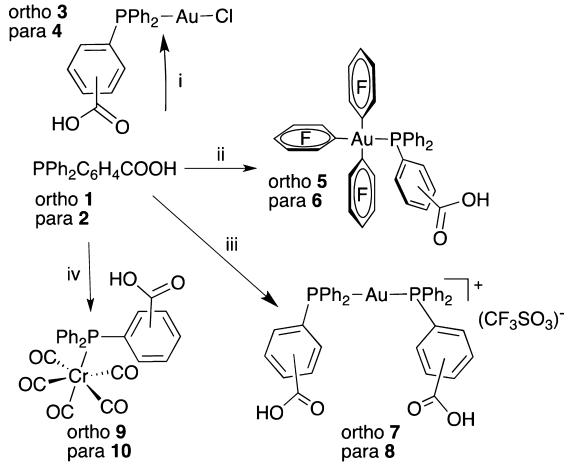

[a](i) [AuCl(tht)]; (ii) [Au$(C_6F_5)_3$(tht)]; (iii) 1/2 [Au(tht)$_2$]CF_3SO_3; (iv) [$Cr(CO)_6$] + Me_3NO.

All complexes display one ν(C═O) band from the carboxylic group in the range 1719−1685 cm^{-1}. The chromium compounds also show carbonyl bands at 2064, 1987, and 1932 cm^{-1}. In their ^{1}H NMR spectra, the aromatic protons of the metallo−organic acids are low-field shifted compared to the free phosphine ligand. The largest shifts are about +0.32 ppm for H^5 in the ortho ligand and +0.40 ppm for H^3 for the para ligand. The assignments given were confirmed by COSY and ^{1}H {^{31}P} NMR. ^{19}F NMR spectra of compounds **5** and **6** show two sets (1:2 ratio) of three resonances (2:1:2 ratio) due to the C_6F_5 groups in the range from −120 to −122 (F_{ortho}), −157 (F_{para}), and −160.5 and −161 ppm (F_{meta}). A singlet at around −79 ppm is observed for the triflate anion of compounds **7** and **8**. The singlet observed in the ^{31}P{^{1}H} NMR spectra is low-field shifted by 23−65 ppm in all complexes compared to the free phosphine ligand.

X-ray Crystal Structure Determination of Complexes 4, 5, 6, and 9. Crystalline structures of **4**, **5**, **6**, and **9** are shown in Figures 2 and 3 with selected bond lengths and angles in Tables 1 and 2. Compounds **4**, **6**, and **9** are dimers through the carboxylic acid groups (bond lengths and angles in Table 3), regardless of the phosphine ortho or para substitution pattern. As expected, the gold(I) complex **4** displays a typical linear coordination for gold, and gold(III) derivatives **5** and **6** show slightly distorted square-planar geometries with standard Au−C, Au−Cl, and Au−P bond distances somewhat longer for gold(III) than for gold(I). The shortest intermolecular Au−Au

dx.doi.org/10.1021/ic501039n | Inorg. Chem. 2014, 53, 10893−10902

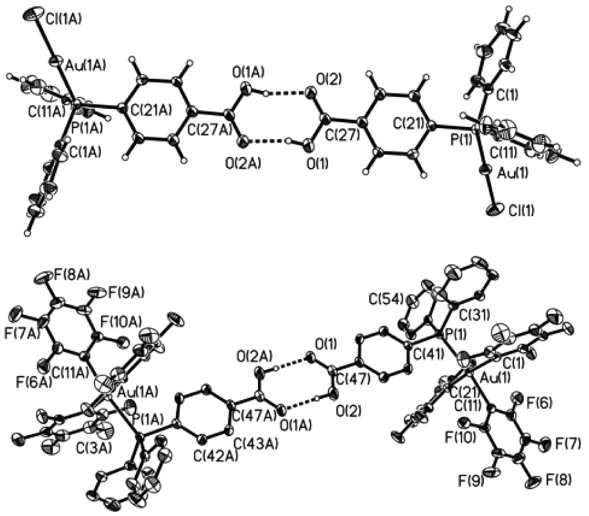

Figure 2. X-ray structures of dimers **4** (top) and **6** (bottom). H atoms omitted for clarity, except for the carboxylic group. Displacement ellipsoids are at the 25% probability level.

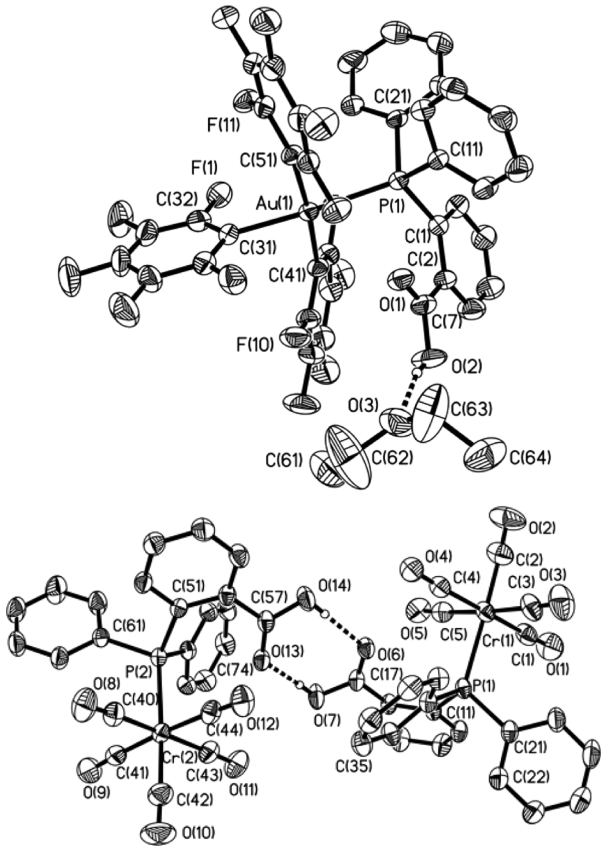

Figure 3. X-ray structure of compounds **5** (top) and **9** (bottom). Displacement ellipsoids are at the 30% probability level. H atoms omitted for clarity, except for the carboxylic group.

distance found for the gold(I) compound **4** is 6.4 Å, which discards any gold−gold interaction. The chromium(0) derivative **9** is also a H-bridged dimer that displays a slightly distorted octahedral geometry for its two independent molecules in the crystal. In contrast to **6**, complex **5** is a monomer with the hydrogen atom of the carboxylic group bonded to the O atom of a cocrystallized diethyl ether molecule. This is due to the high steric requirement of the $Au(C_6F_5)_3$ fragment embedding the acid group, which precludes ortho dimerization but not para dimerization. All compounds show two different C−O bond lengths in the carboxylic functional group (Table 1). A review in the literature reports that formation of a carboxylic acid dimer requires the absence of competitors, and in the known X-ray structure only about 29% of the compounds form the classic dimer, whereas the remaining 71% form hydrogen bonds with a large variety of other acceptors.[22]

Hydrogen-Bonded Triazine−[M] Adducts. Triazine (**T**) was reacted with the diphenylphosphinobenzoic acid ligands **1** and **2** and the metal complexes **3**−**10** in THF in the appropriate molar ratio (1:1 or 2:1, depending on the number of acid groups in the complex), followed by slow evaporation of the solvent (Scheme 2). This afforded pale brown (free phosphines and gold) or green (chromium) waxy solids, which were then studied to see whether they correspond to defined $\mathbf{T}^n$ adducts or not.

The waxy materials obtained in the reactions aimed at producing supramolecular hydrogen-bonded adducts were examined by several techniques to find out their nature and thermal properties. They can be classified in three groups: (1) mixtures of the reactants, (2) hydrogen-bonded adducts, and (3) uncertain materials. To the first group pertain the gold(III) materials $\mathbf{T}^5$ and $\mathbf{T}^6$, which show clearly, at room temperature in polarized optical microscopy (POM), a mixture of crystals and liquid, indicating that the corresponding adducts have not been formed. The rest of the compounds apparently show mesophases at room temperature but with very different thermal behavior. $\mathbf{T}^2$, $\mathbf{T}^4$, $\mathbf{T}^8$, and $\mathbf{T}^{10}$ resist some heating maintaining the mesophase texture until the clearing point is reached; moreover, as discussed in detail later, small-angle powder X-ray diffraction (SAXS) studies support formation of columnar mesophases by these hydrogen-bonded supramolecular adducts. Finally, whether the triazine forms or not adducts $\mathbf{T}^1$, $\mathbf{T}^3$, $\mathbf{T}^7$, and $\mathbf{T}^9$ is doubtful, and their nature is uncertain. Only $\mathbf{T}^9$ displays IR (ν(C≡O)) and SAXS data that might support formation of the adduct: the A_1 mode associated mainly to the CO trans to the phosphine group diminishes clearly in intensity and shifts +8 (for $\mathbf{T}^9$) or +10 cm^{-1} (for $\mathbf{T}^{10}$, see Figure S1, Supporting Information). The same behavior was observed in closely related adducts.[13] The fact that $\mathbf{T}^9$ and $\mathbf{T}^{10}$ give quite similar shifts seems to suggest that not only $\mathbf{T}^{10}$ but also $\mathbf{T}^9$ might be an adduct.[23] The others ($\mathbf{T}^1$, $\mathbf{T}^3$, $\mathbf{T}^7$) quickly decompose under the X-ray observation, with formation of crystals of the starting acid, so their thermal behavior looks uninteresting.

Overall, the results suggest that the stability of the H-bonded adducts versus their separated components is modest and structural variations in the components are critical. Thus, aspects such as the size of the metallic moiety (as in $\mathbf{T}^5$ and $\mathbf{T}^6$) or the angle made at the acid ring (2- versus 4-diphenylphosphinobezoic) will determine whether the supramolecular material will be formed or not. The stability of the H-bonded adducts is not very high even for the materials that undoubtedly form adducts and mesophases, and diffusion-ordered NMR spectroscopy (DOSY) shows that in $CDCl_3$, acetone-d_6, or in THF-d_8 solution $\mathbf{T}^2$, $\mathbf{T}^4$, $\mathbf{T}^8$, and $\mathbf{T}^{10}$ are dissociated into their components. (see Figure S2, Supporting Information). Thus, formation of a condensed phase is critical for formation of adducts.

Thermal Behavior. The thermal behavior of the supramolecular adducts was investigated by differential scanning

dx.doi.org/10.1021/ic501039n | Inorg. Chem. 2014, 53, 10893−10902

Table 1. Selected Bond Lengths (Angstroms) and Angles (degrees) for Complexes 3, 4, 5, and 6

	3[a]	4[b]	4	5	6
Au−P	2.26(1)	2.232(4), 2.225(4)[c]	2.2249(19)	2.3808(18)	2.3768(13)
Au−Cl	2.29(1)	2.278(4), 2.269(4)	2.271(2)		
Au−C				2.070(7), 2.079(7), 2.109(7)	2.068(5), 2.073(5), 2.077(5)
O═C	1.24(4)	1.24(2), 1.21(2)	1.245(9)	1.211(10)	1.239(6)
O−C	1.34(3)	1.29(2), 1.30(2)	1.283(9)	1.329(9)	1.292(7)
P−Au−Cl	172.9(4)	177.5(1), 178.9(1)	178.75(8)		
P−Au−C				176.2(2), 90.86(19), 94.0(2)	171.50(16), 91.58(14), 93.43(14)
C−Au−C				175.1(3), 87.9(3), 87.2(3)	173.45(19), 87.72(19), 87.95(19)
O−C−O	125(4)	124(1), 125(1)	122.1(8)	124.5(8)	124.4(5)

[a]Data from ref 19. [b]Data from ref 18. [c]Two independent molecules.

Table 2. Selected Bond Lengths (Angstroms) and Angles (degrees) for Compound 9

Cr(1)−P(1)	2.3985(9)	C(2)−Cr(1)−P(1)	176.65(14)
Cr(1)−C(1)	1.894(3)	C(1)−Cr(1)−C(4)	177.22(15)
Cr(1)−C(2)	1.861(4)	C(3)−Cr(1)−C(5)	176.65(17)
Cr(1)−C(3)	1.888(4)	O(1)−C(1)−Cr(1)	178.0(4)
Cr(1)−C(4)	1.900(3)	O(2)−C(2)−Cr(1)	177.7(5)
Cr(1)−C(5)	1.889(4)	O(3)−C(3)−Cr(1)	176.9(4)
C(1)−O(1)	1.128(4)	O(4)−C(4)−Cr(1)	176.8(3)
C(17)−O(6)	1.207(3)	O(5)−C(5)−Cr(1)	176.6(3)
C(17)−O(7)	1.319(3)	O(6)−C(17)−O(7)	123.2(2)

Table 3. Hydrogen Bonds Involving the Carboxylic Group for Dimers 4, 6, and 9 and Monomer 5 (Angstroms and degrees)[a]

D−H···A	d(D−H)	d(H···A)	d(D···A)	<(DHA)
compound **4**				
O(1)−H(1)···O(2A)	0.820	1.808	2.594	160.09
O(1A)−H(1A)···O(2)	0.820	1.808	2.594	160.09
compound **6**				
O(2)−H(2)···O(1A)	0.820	1.814	2.631	174.97
O(2A)−H(2A)···O(1)	0.820	1.814	2.631	174.97
compound **9**				
O(7)−H(7)···O(13)	0.820	1.857	2.676	175.61
O(14)−H(14A)···O(6)	0.820	1.878	2.698	179.08
compound **5**				
O(2)−H(2)···O(3)	0.821	1.825	2.626	164.89

[a]Symmetry transformations used to generate equivalent atoms: for compound **4** $-x+1, -y-1, -z$; for compound **6** $-x, -y+2, -z+1$.

Scheme 2. Reactions for Synthesis of Supramolecular Triazine−Metalloacid Adducts, T^{n}[a]

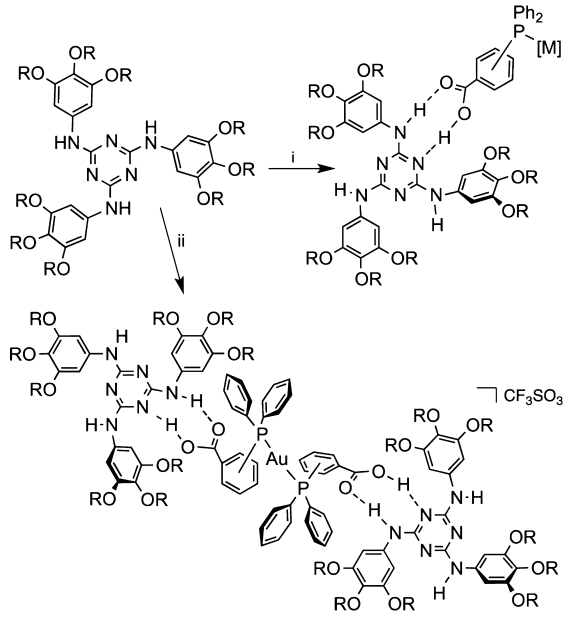

[a]H-bonding system is indicated by dashed lines. R = $C_{10}H_{21}$. Attempted syntheses are (i) reactions with compounds **1**−**6**, **9**, and **10**; (ii) the same with compounds **7** and **8**.

calorimetry (DSC), POM, and SAXS. The triazine used in this work,[24] bearing nine diverging decyloxy chains, displays a columnar hexagonal mesophase (Col_{hex}) from room temperature to 57 °C, when it clears reversibly to the isotropic liquid.[13,14] The diphenylphosphinobenzoic acid derivatives **1** and **2** and metallo−organic acid complexes **3**−**10** are not mesomorphic. Compound **10** and the free phosphines **1** and **2** have melting points in the range 87−175 °C, but complexes **3**−**9** decompose without melting in the range 162−250 °C. Remarkably, all supramolecular adducts derived from *p*-diphenylphosphinobenzoic acid are liquid crystals at room temperature (Table 4). Fluid and homogeneous optical textures could be observed by POM for these adducts: sandy-like textures for the phosphine adduct T^2 and for the chromium adduct T^{10}; ill-defined pseudo-fan-shaped texture with some dark (homeotropic) regions for T^4 and T^8 (Figure 4). These textures, although nonspecific, unambiguously confirm a mesophase for these four adducts that is compatible with a hexagonal columnar arrangement.

This thermal behavior was confirmed by DSC measurements (Table 4, Supporting Information Figure S4). T^4, T^8, and T^{10} behave as classical enantiotropic liquid crystals. For T^2 the columnar mesophase formed during the first cooling is maintained at room temperature over several days. With respect to the parent triazine, the mesophase-to-isotropic liquid transition temperature (second heating) is very similar for the gold(I) compounds T^4 (ca. +2 °C) and T^8 (ca. −2 °C) and lower for compounds T^2 and the chromium(0) T^{10} (about −20 °C). No sign of crystallization or glass transition was detected on cooling the samples to −20 °C, but they became much less fluid and looked frozen, suggesting that a glassy state had been reached. Heating well above the clearing point produced adduct decomposition to give some microcrystals of the starting metallo−organic acids and free triazine. Only a very small difference in transition temperature is observed between the triazine and the corresponding gold adducts (T^4 and T^8). The same somewhat unpredicted behavior was found in our previous study with related gold adducts.[14] We explain this

dx.doi.org/10.1021/ic501039n | Inorg. Chem. 2014, 53, 10893−10902

Table 4. Optical, Thermal, and Thermodynamic Data of Triazine (T) and Adducts (T^n)

compd	transition[a]	T/°C[b]	ΔH^b/J g^{-1}
T	Col_{hex} → I	H1:57.1	2.0
	I → Col_{hex}	C1:42.6	1.1
	Col_{hex} → I	H2:57.5	1.2
T^1	dissociated[c]	H1:37.4	
T^2	Cr → I	H1:51	11.2
	I → Col_{hex}	C1:29.5	1.7
	Col_{hex} → I	H2:35.8	1.7
T^3	dissociated[c]	H1:40.7	
T^4	Col_{hex} → I	H1:60.0	1.2
	I → Col_{hex}	C1:51.6	1.3
	Col_{hex} → I	H2:59.6	1.3
T^7	dissociated[c]	H1:40	
T^8	Col_{hex} → I	H1:55.6	1.3
	I → Col_{hex}	C1:29.5	1.0
	Col_{hex} → I	H2:55.4	1.1
T^9	dissociated[c]	H1:52.5	
T^{10}	Col_{hex}[d] → I	H1:38.3	2.5
	I → Col_{hex}	C1:18.1	2.7
	Col_{hex} → I	H2:35.7	3.7

[a]Cr, crystalline phase; Col_{hex}, columnar hexagonal phase; I, isotropic liquid. [b]H1, H2, C1: first and second heating and first cooling; temperature corresponds to the peak maximum. [c]Dissociated means that the adducts are split into their triazine and metalloacid components upon heating above the temperature mentioned. [d]A lamellar arrangement cannot be fully excluded.

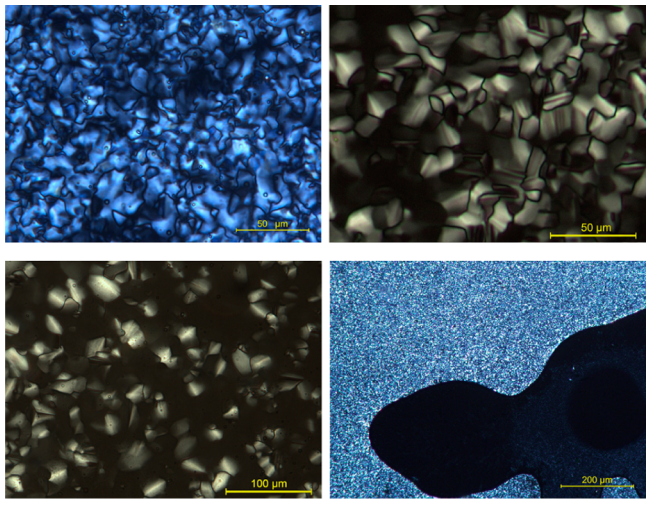

Figure 4. Polarized optical microscopic texture observed for the free triazine **T** (top left) and for adducts $\mathbf{T}^4$ (top, right), $\mathbf{T}^8$ (bottom left), and $\mathbf{T}^{10}$ (bottom right) obtained on cooling from isotropic liquid at room temperature. Enlarged pictures are available in Supporting Information Figure S3.

similarity assuming that the metal complex moieties are somehow buried into the dominant aliphatic environment of the azine chains in such a way that each discotic unit of adduct appears externally very similar to the triazine discs. In fact, the mesophases of **T** and $\mathbf{T}^n$ (n = 2, 4, 8, 10) mix perfectly in contact experiments. In contrast, addition of additional metal complex to $\mathbf{T}^n$ systems does not result in mixing, providing further evidence for specific adduct formation.

Further information and elucidation of the mesophases observed comes from studies of small-angle powder X-ray diffraction as a function of temperature, covering from room temperature up to the isotropic liquid. The supramolecular aggregates show limited stability under prolonged exposure to X-ray beam and temperature. Unambiguous assignment of the mesophases needed, however, access to more small reflections than visible in the diffractograms acquired with conventional laboratory sources. These missing reflections could be acquired on a synchrotron SAXS line. Diffractograms of the adducts containing 4-diphenylphosphinobenzoic acid as linker, $\mathbf{T}^2$, $\mathbf{T}^4$, $\mathbf{T}^8$, and $\mathbf{T}^{10}$, exhibit at least two common characteristic features: (i) in the small-angle region, one sharp and intense reflection along, in some cases, with additional weaker reflections, which are indicative of long-range ordered low-dimensional lattices, and (ii) in the large-angle region, one broad, very strong, scattering halo spreading between 3.5 and 5.5 Å (intensity maximum at about 4.4−4.6 Å), corresponding to the overlap of different, undifferentiated, lateral distances between aliphatic tails and between adduct fragments (undifferentiated h_{ch} + h_{adduct}, Table 5). In all cases, the fundamental reflection dominates over the higher order reflections and is due to the strong density contrast arising from the alternation of electron-rich columns and electron-poor fluid and continuous zones. This contrast is further enhanced by the presence of the metallic ion within the columns and logically reduces the higher order reflections (therefore the need to use a highly intense source like synchrotron).

The diffractogram of the phosphine adduct $\mathbf{T}^2$ confirms formation of a columnar hexagonal mesophase close to 40 °C: it displays the strong and diffuse wide-angle scattering typical of the molten aliphatic chains and cores, along four sharp, small-angle reflections, in the square spacing ratio $1:\sqrt{3}:2:\sqrt{7}$, which were, respectively, indexed as to the (10), (11), (20), and (21) reflections of a hexagonal lattice with a parameter of 29.05 Å (Figure 5 and Table 5). On further heating above the isotropization (at T = 65 °C) the supramolecular adduct partially dissociates into its elementary components as evidenced by the superposition of the diffraction peaks associated with both the free triazine in its mesophase and the phosphine acid **2** in its crystalline state (Supporting Information, Figure S5). The adduct reforms readily and recrystallizes on cooling to 25 °C. It shows a reversible behavior only when heated below the clearing transition.

The adduct $\mathbf{T}^4$ exhibits a Col_{hex} mesophase at room temperature in a temperature range similar to that of **T**. Diffractograms (Figure 6, Supporting Information Figure S5) recorded at 25 and 50 °C indeed show two or three sharp small-angle reflections of the hexagonal lattice, the broad scattering of the molten chains and cores, as well as an additional diffuse weak halo at midangle arising likely from short-range metal−metal interactions within the columnar structure. Thus, connection of the [AuCl] fragment onto the phosphine modifies and enhances the mesophase stability with respect to the nonmetallic structurally related $\mathbf{T}^2$ compound. Actually, the presence of the metallic fragment is associated with a slight contraction of the hexagonal cell (Table 5). Similarly, mesomorphism is maintained in the corresponding dimeric adduct ($\mathbf{T}^8$): $\mathbf{T}^8$ is mesomorphic at room temperature, and SAXS revealed unequivocally formation of a Col_{hex} phase, deduced from the presence of the two small-angle reflections indexed as (10) and (11) of a hexagonal lattice (Figure 6, Supporting Information Figure S5). The chromium adduct $\mathbf{T}^{10}$ shows mesomorphism, but only in a narrow range around room temperature (Figure 6). Although the nature of the mesophase

dx.doi.org/10.1021/ic501039n | Inorg. Chem. 2014, 53, 10893−10902

Table 5. Geometrical Parameters of Mesophases Obtained from SAXS for the T^n Adducts[a]

compound	T/°C	q/Å^{-1}	d/Å	hk	I	a/Å	S/Å^2	V_{mol}/Å^3	h_{adduct}/Å
triazine	30		25.83	10	VS(sh)	29.82	770	2966	3.85
T^2	40	0.2498	25.15	10	VS(sh)	29.05	731	3432	4.69
		0.4320	14.54	11	W(sh)				
		0.4997	12.57	20	VW(sh)				
		0.6608	9.51	21	W(sh)				
T^4	25	0.2550	24.64	10	VS(sh)	28.46	701	3845	5.48
		0.4412	14.24	11	W(sh)				
T^8	20		25.70	10	VS (sh)	29.7	764	7440	4.87
			14.85	11	VW (sh)				
T^{10}	20		26.0	10	VS (sh)	30.1	780	3752	4.81

[a] T = temperature of the experiment; q = wave vector ($q = 2\pi/d$); d = d spacing; hk = Miller indices; I = reflection intensity (VS, very strong; W, weak; VW, very weak; sh: sharp); a = hexagonal lattice parameter; S = cross-columnar section area ($S = A^2\sqrt{3}/2$); V_{mol} = molecular volume (triazine and adducts); h_{adduct} = molecular height per adduct ($h_{adduct} = V_{mol}/SN$, where N is the number of triazines per complex, e.g., $N = 1$ for monomers, $N = 2$ for dimers).

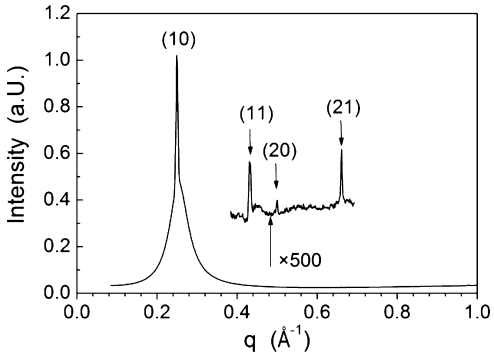

Figure 5. SAXS diffractogram (synchrotron) of adduct **T^2** at ca. 40 °C, after cooling from isotropic liquid.

cannot be unequivocally assigned on the basis of the unique visible reflection, the analogy with the other structurally related adducts **T^4** and **T^8**, and the overall similar trends observed with their mesomorphic behavior reasonably support assigning the mesophase as Col_{hex} too. A lamellar arrangement cannot be fully excluded.

As commented above, reaction between the gold(III)-based acids (**5** or **6**) and triazine does not proceed and thus does not yield wanted adducts **T^5** or **T^6**. Diffractograms of the binary mixture **T**+**6** (recorded at 25 °C in the pristine state, 55 °C, and then back at 25 °C; see Supporting Information, Figure S5) confirm nonformation of the H-bonded adduct, as evidenced by the superposition of the distinct signals of each species, namely, the sharp small-angle reflection of **T** in the Col_{hex} (T = 25 °C), which broadens when entering in the isotropic phase (T = 55 °C), and the numerous sharp reflections scanning the entire diffraction angle range of **6** in the crystalline state (at all temperatures).

For the materials containing 2-diphenylphosphinobenzoic acid complexes the results are very different. The material labeled **T^3** (**T** + **3**) appears immediately dissociated upon heating and on beam exposure as shown by SAXS, which reveals phase coexistence between solid free phosphine acid and pure triazine in its mesophase (Supporting Information, Figure S5). **T^7** (**T** + **7**) and **T^9** (**T** + **9**) (Supporting Information, Figure S5) show a similar behavior.

In summary, mesomorphism is exclusively observed for the analogous *p*-[M]−phosphine adducts, suggesting that the metallo−organic acids again play the role of a fourth arm of the triazine, thus filling the empty regions between the arms

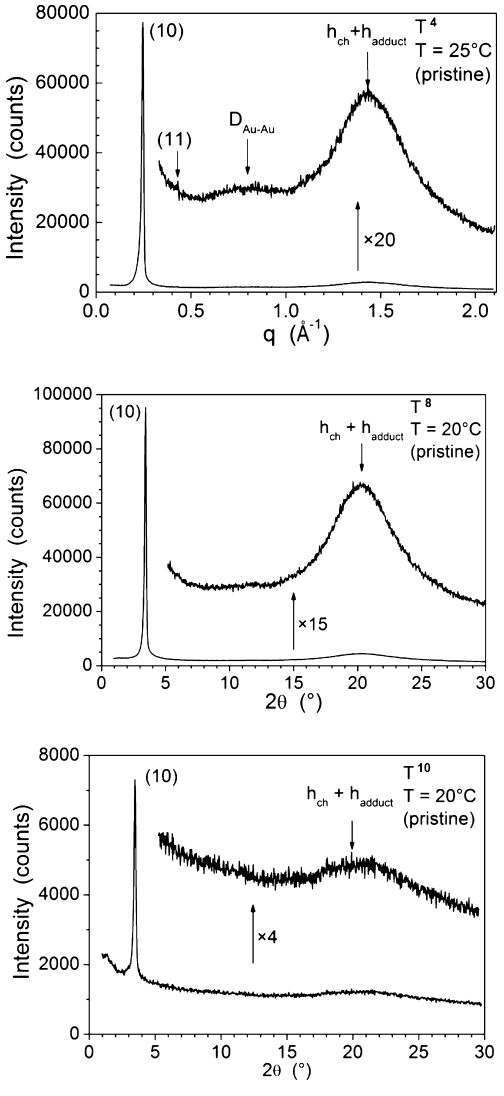

Figure 6. X-ray diffraction patterns for (a) **T^4** at 25 °C, (b) **T^8** at 20 °C, and (c) **T^{10}** at 20 °C.

and smoothing the columnar interface.[14] The columnar phase results from the stacking of these pseudo-discotic adducts into columns with a slight elongation of each unit (disc) when passing from the triazine to the adducts (see h_{adduct} values in Table 5). Unlike other triazine thiolatobenzoic acid systems

dx.doi.org/10.1021/ic501039n | Inorg. Chem. 2014, 53, 10893−10902

reported before,[14] none of the ortho systems exhibits mesomorphic properties, probably because adducts have not been formed. The weakness (T^4) or absence of the diffuse signal previously observed for the thiolatobenzoic acid compounds at midangle suggests that the metallic ions are essentially camouflaged within the branch of the triazine with little interactions between neighbors and without protruding in the aliphatic continuum. This difference may be ascribed to the different geometry around the P and S atoms, respectively. The tetrahedral geometry around the P atom of the phosphine group will keep the metallic fragment closer to the columnar core due to the bent angle at P, whereas the diverging phenyl entities will be partly mixed with the aromatic parts forming the columnar cores and the aliphatic chains, without dramatically changing the distribution of the electronic density, as was the case for the thiolatobenzoic acid systems having a closer to linear geometry around the S atom. Obviously, the ortho position does not allow for such arrangement and on the contrary will disrupt the packing of adducts along the columns.

Photophysical Behavior. Emission and excitation spectra of the free phosphine and metallo−organic acids were recorded in the solid state at 77 or 298 K and in CH_2Cl_2 frozen solution at 77 K. None of them emits in solution at 298 K. Emission and excitation spectra of the supramolecular adducts (T^2, T^4, T^8, T^{10}) were recorded in the solid state at 77 or 298 K. Spectra of complex **8** and adduct T^8 at 77 K are shown as representative examples in Figure 7. Details of the excitation and emission spectra are given in Tables S1 and S2, Supporting Information.

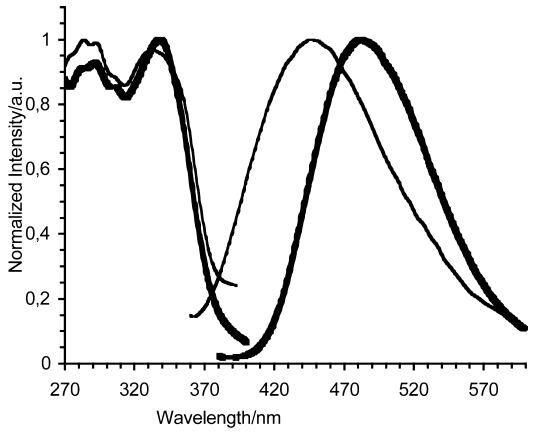

Figure 7. Excitation and emission spectra of **8** (bold line) and T^8 (normal line) dispersed in KBr at 77 K. Note that the plot is in normalized intensity. This produces a deceptive appearance of identical intensity for the two compounds.

4-Diphenylphosphinobenzoic acid and all the gold metalloacids are emissive at 77 K in the range 404−520 nm and some of them also at 298 K with emission maxima from 441 to 485 nm. However, neither the chromium compounds **9** and **10** nor the free 2-diphenylphosphinobenzoic acid show any emission in this range. Consequently, this emission is associated with the Au−P(acid) fragment. Many gold(I) compounds are luminescent in the visible region,[25] but luminescent gold(III) compounds are comparatively scarce.[26]

All adducts emit and show, at 77 K, a structureless broad emission band in the range 419−455 nm, which appears not only for the complexes containing the Au−P(acid) fragment but also for the chromium adduct T^{10} and the free ligand adduct T^2. Moreover, this emission appears within a narrow range in spite of the modifications in the metallic fragment and also close to a strong emission of the free triazine, which appears at 423 nm. Thus, the conclusion is that this emission in the adducts is triazine centered, and the expected phosphine- or Au−P-centered emissions in T^2, T^4, and T^8 are of lower intensity and overlapped by the azine-centered emission.

■ CONCLUSIONS

2-Diphenylphosphinobenzoic and 4-diphenylphosphinobenzoic acids behave toward metal centers as typical monodentate phosphine ligands do. Thus, gold(I) or gold(III) and chromium(0) complexes have been prepared. The free carboxylic functional groups of these two phosphine acids or their metallo−organic acids produce H-bridged dimers, except for the *o*-phosphine gold(III) complex because of its voluminous substituents at gold. They can also form donor−acceptor adducts with an appropriate triazine, providing some *p*-phosphine chromium(0) and gold(I) metalloacid−triazine supramolecular adducts that display stable hexagonal columnar mesophases at room temperature. In the columnar stacking of adducts the metallic fragment finds room to accommodate itself as a wedge filling the space between the branches of the trefoil molecular architecture of the triazine units. This is an example showing how the triazine bearing nine lateral alkoxy chains manages to accommodate pretty large metal−organic fragments to produce adducts without losing the mesomorphic behavior. However, the very unfavorable sterics of the *o*-phosphine metalloacids is clearly detrimental for formation of adducts with the triazine. It is doubtful whether they really form at all adducts or simply their adducts do not stand moderate temperatures close to room temperature or X-ray irradiation. The Achilles heel of the supramolecular entities discussed here is the weakness of the connection of the two components, the hydrogen bond. Otherwise, it looks like that with heavily alkyl-substituted azines pretty unfavorable geometries and fairly voluminous groups can be accommodated into discoid products that display mesophases at low temperature with a columnar order.

■ EXPERIMENTAL SECTION

General procedures are as reported before.[14] ^1H, ^{19}F, and $^{31}P\{^1H\}$ NMR chemical shifts are quoted relative to $SiMe_4$ (external, ^1H), $CFCl_3$ (external, ^{19}F), and 85% H_3PO_4 (external, ^{31}P). Emission and excitation spectra at 298 and 77 K were measured in the solid state as finely pulverized KBr mixtures and in deoxygenated CH_2Cl_2 solutions (about 10^{-3} M) in quartz tubes with a Perkin-Elmer LS-55 spectrofluorimeter. For characterization of the LC mesophases, in addition to POM and DSC, small-angle X-ray scattering techniques were used. Variable-temperature small-angle X-ray patterns were obtained using a linear focalized monochromatic Cu Kα1 beam (λ = 1.5405 Å) using a sealed-tube generator (900 W) equipped with a bent quartz monochromator. In all cases, the crude powder was filled in thin Lindemann capillaries of 1 mm diameter and 10 μm wall thickness in air (corrections for air were made) and then heated to produce the mesophase. An initial set of diffraction patterns was recorded with a curved Inel CPS 120 counter gas-filled detector linked to a data acquisition computer; periodicities up to 70 Å can be measured and the sample temperature controlled to within ±0.01 °C from 20 to 200 °C. Alternatively, patterns were also recorded on an image plate; periodicities up to 120 Å can be measured (scanned by STORM 820 from Molecular Dynamics with 50 mm resolution). For some samples, synchrotron patterns were obtained on the SWING synchrotron beamline in the SAXS configuration at 12 keV energy (proposal 20120951) using a homemade transmission oven of 0.1 °C accuracy and filling samples in 1 mm Lindemann capillaries.

Table 6. Details of Crystallographic Data and Structure Refinement for Acids 4, 5, 6, and 9

	4	5·Et_2O·H_2O	6·$CHCl_3$	9·0.25hexane
empirical formula	$C_{19}H_{15}AuClO_2P$	$C_{41}H_{15}AuF_{15}O_4P$	$C_{38}H_{16}AuCl_3F_{15}O_2P$	$C_{25.50}H_{15}CrO_7P$
fw	538.70	1084.47	1123.79	516.34
temp (K)	293(2)	293(2)	293(2)	293(2)
wavelength (Å)	0.71073	1.54184	0.71073	1.54184
cryst syst	monoclinic	monoclinic	triclinic	triclinic
space group	$P2(1)/c$	$P2(1)/c$	$P-1$	$P-1$
unit cell dimens: a (Å)	18.9328(5)	14.4299(2)	9.8540(8)	10.9729(5)
b (Å)	7.12915(16)	15.2743(3)	10.4075(4)	14.6769(7)
c (Å)	16.7656(4)	18.6396(4)	19.2765(17)	15.7818(8)
α (deg)	90	90	92.533(5)	78.135(4)
β (deg)	94.008(2)	98.8129(19)	99.200(7)	74.224(4)
χ (deg)	90	90	93.152(5)	88.521(4)
vol. (Å^3)	2257.40(10)	4059.79(14)	1945.7(2)	2392.4(2)
Z	4	4	2	4
density (calcd) (Mg/m^3)	1.585	1.774	1.918	1.434
abs coeff (mm^{-1})	6.712	8.194	4.135	4.951
F(000)	1024	2088	1080	1052
cryst habit	needle	plate	plate	plate
cryst size (mm)	0.32 × 0.05 × 0.05	0.26 × 0.13 × 0.08	0.27 × 0.19 × 0.07	0.29 × 0.19 × 0.08
Θ range for data colln	2.16−28.68	3.10−75.15	2.10−28.76	2.97−75.08
index ranges	$-21 \le h \le 24$, $-6 \le k \le 9$, $-22 \le l \le 12$	$-17 \le h \le 16$, $-18 \le k \le 12$, $-23 \le l \le 22$	$-12 \le h \le 9$, $-7 \le k \le 13$, $-23 \le l \le 22$	$-13 \le h \le 6$, $-18 \le k \le 18$, $-19 \le l \le 18$
no. of reflns collected	9039	12 575	13 316	14 476
no. of independent reflns	4774 [R(int) = 0.0258]	7959 [R(int) = 0.0338]	8046 [R(int) = 0.0260]	9356 [R(int) = 0.0247]
max and min trans.	0.752 and 0.525	0.601 and 0.349	0.796 and 0.450	0.720 and 0.480
data/restraints/params	4774/0/205	7959/0/559	8046/0/541	9356/0/622
goodness-of-fit on F^2	1.115	1.021	1.041	1.025
final R indices [$I > 2\sigma(I)$]	R1 = 0.0447, wR2 = 0.1296	R1 = 0.0457, wR2 = 0.1198	R1 = 0.0391, wR2 = 0.0869	R1 = 0.0409, wR2 = 0.1070
R indices (all data)	R1 = 0.0686, wR2 = 0.1421	R1 = 0.0781, wR2 = 0.1397	R1 = 0.0504, wR2 = 0.0937	R1 = 0.0595, wR2 = 0.1215
largest difference peak and hole (e·Å^{-3})	1.429 and −0.649	1.089 and−1.470	1.113 and−1.018	0.391 and−0.330

Synthesis of the Precursors. [AuCl(tht)],[27] [Au(C_6F_5)$_3$(tht)],[28] [Ag(CF_3SO_3)(tht)],[29] and [{($C_{10}H_{21}O$)$_3$$C_6H_2$NH}$_3$$C_3N_3$][12] were prepared according to literature methods. The other reagents were obtained from commercial sources.

*Synthesis of [AuCl(PPh$_2$C$_6$H$_4$CO$_2$H)] (ortho (**3**) and para (**4**)) and [Au(C$_6$F$_5$)$_3$(PPh$_2$C$_6$H$_4$CO$_2$H)] (ortho (**5**) and para (**6**)).* To a dichloromethane solution (20 mL) of [AuX$_n$(tht)] (100 mg; X = Cl, n = 1, 0.31 mmol for the synthesis of **3** and **4**; X = C_6F_5, n = 3, 0.13 mmol for the synthesis of **5** and **6**) was added the corresponding diphenylphosphinobenzoic acid **1** or **2** (96 mg, 0.31 mmol, for synthesis of **3** and **4**; 40 mg, 0.13 mmol, for synthesis of **5** and **6**), and the reaction was stirred at room temperature for 90 min. The solution was then concentrated to ca. 5 mL. Addition of hexane afforded compounds **3**−**6** as white solids. Compound **5** was purified from the starting materials by crystallization from chloroform/diethyl ether mixture. Yield of **3**: 134 mg, 80%. Mp: 205 (dec.). Anal. Calcd: C, 42.36; H, 2.81; N, 0. Found: C, 42.55; H, 2.71; N, 0. ^{1}H NMR (d_6-acetone, 400 MHz): δ_H 7.02 (ddd, J_{HP} = 12.7 Hz, J_{HH} = 7.79 and 1.1 Hz 1H, H^3), 7.60−7.53 (m, 10H, H$_o$, H$_p$, and H$_m$), 7.69 (tt, J_{HH} = 7.8 and 1.7 Hz, J_{HP} = 1.7 Hz, 1H, H^4), 7.79 (tt, J_{HH} = 7.7 and 1.5 Hz, J_{HP} = 1.5 Hz, 1H, H^5), 8.34 (ddd, J_{HH} = 7.5 and 1.6 Hz, J_{HP} = 4.4 Hz, 1H, H^6). ^{31}P{^{1}H} NMR (d_6-acetone, 162 MHz): δ_P 37.49 (s). IR (KBr): 3062 ν(O−H), 1685 ν(C═O) cm^{-1}. Yield of **4**: 140 mg, 84%. Mp: 200 (dec.). Anal. Calcd: C, 42.36; H, 2.81; N, 0. Found: C, 41.97; H, 2.74; N, 0. ^{1}H NMR (d_6-acetone, 400 MHz): δ_H 7.67−7.61 (m, 10H, Ph), 7.73 (dd, J_{HH} = 7.9 and J_{HP} =12.7 Hz, 2H, H^3), 8.20 (dd, J_{HH} = 7.9 and J_{HP} = 2.2 Hz, 2H, H^2). ^{31}P{^{1}H} NMR (d_6-acetone, 162 MHz): δ_P 34.34 (s). IR (KBr): 3062 ν(O−H), 1694 ν(C═O) cm^{-1}. Yield of **5**: 38 mg, 29%. Mp: 210 (dec.). Anal. Calcd: C, 44.24; H, 1.51; N, 0. Found: C, 44.46; H, 1.98; N, 0. ^{1}H NMR ($CDCl_3$, 400 MHz): δ_H 6.97 (dd, J_{HH} = 7.8 Hz, J_{HP} = 13.0 Hz, 1H, H^3), 7.34−7.63 (m, 12H, Ph + H^4 + H^5), 8.17 (dd, J_{HP} = 4.5 Hz, J_{HH} = 7.2 Hz, 1H, H^6). ^{19}F NMR ($CDCl_3$, 376 MHz): δ_F −119.5 (brm, 4F, F$_o$−Au), −121.7 (m, 2F, F$_o$−Au), −157.1 (t, N = 18.0 Hz, 3F, F$_p$−Au), −160.7 (m, 4F, F$_m$−Au), −161.2 (m, 2F, F$_m$−Au). ^{31}P{^{1}H} NMR ($CDCl_3$, 162 MHz): δ_P 23.9 (s). IR (KBr): 3087 ν(O−H), 1689 ν(C═O), 970, 804, 792 (C_6F_5) cm^{-1}. Yield of **6**: 95 mg, 73%. Mp: 240 (dec.). Anal. Calcd: C, 44.24; H, 1.51; N, 0. Found: C, 44.46; H, 1.98; N, 0. ^{1}H NMR ($CDCl_3$, 400 MHz): δ_H 7.44−7.47 (m, 8H, H^m and H^o of Ph), 7.53 (dd, J_{HH} = 8.5 and J_{HP} = 11.7 Hz, 2H, H^3), 7.60 (m, 2H, H^p of Ph), 8.10 (dd, J_{HH} = 8.5 and J_{HP}= 2.5 Hz, 2H, H^2). ^{19}F NMR ($CDCl_3$, 376 MHz): δ_F −119.9 (m, 4F, F$_o$−Au), −121.7 (m, 2F, F$_o$−Au), −156.6 (t, N = 18.8 Hz, 2F, F$_p$−Au), −156.7 (t, N = 19.4 Hz, 1F, F$_p$−Au), −160.5 (m, 4F, F$_m$−Au), −160.8 (m, 2F, F$_m$−Au). ^{31}P{^{1}H} NMR ($CDCl_3$, 162 MHz): δ_P 18.1 (s). IR (KBr): 3066 ν(O−H), 1702 ν(C═O), 969, 804 sh, 795 (C_6F_5) cm^{-1}.

*Synthesis of [Au(PPh$_2$C$_6$H$_4$CO$_2$H)$_2$](CF$_3$SO$_3$) (ortho (**7**) and para (**8**)).* To an acetone (20 mL) solution of [AuCl(tht)] (50 mg, 0.156 mmol) was added [Ag(CF_3SO_3)(tht)] (54 mg, 0.156 mmol), and the mixture was stirred at room temperature for 1 h protected from the light. Precipitate of AgCl was filtered off. The corresponding diphenylphosphinobenzoic acid (**1** or **2**: 96 mg, 0.31 mmol) was added to the solution. After stirring for 1 h, the solution was concentrated to ca. 5 mL. Addition of hexanes afforded compounds **7** and **8** as white solids. Yield of **7**: 129 mg, 86%. Mp: 219 (dec.). Anal. Calcd: C, 48.86; H, 3.15; N, 0. Found: C, 48.56; H, 3.30; N, 0. ^{1}H NMR (d_6-acetone, 400 MHz): δ_H 7.07 (ddd, J_{HH} = 7.9 and 1.3, J_{HP} = 12.9 Hz, 1H, H^3), 7.62−7.55 (m, 10H, Ph), 7.71 (tt, J_{HH} = 7.6 and 1.6, J_{HP} = 1.6 Hz, 1H, H^4), 7.81 (tt, J_{HH} = 7.6 and 1.5, J_{HP} = 1.5 Hz, 1H, H^5), 8.39 (ddd, J_{HH} = 7.9 and 1.4, J_{HP} = 4.4 Hz, 1H, H^6). ^{19}F NMR (d_6-acetone, 376 MHz): δ_F −79.3 (s). ^{31}P{^{1}H} NMR (d_6-acetone, 162 MHz): δ_P 47.4 (s). IR (KBr): 3058 ν(O−H), 1702 ν(C═O), 1225, 636 (CF_3SO_3) cm^{-1}. Yield of **8**: 72 mg, 48%. Mp: 162 (dec.). Anal. Calcd: C, 48.86; H, 3.15; N, 0. Found: C, 48.80; H, 3.49; N, 0. ^{1}H

dx.doi.org/10.1021/ic501039n | Inorg. Chem. 2014, 53, 10893−10902

NMR (d_6-acetone, 400 MHz): δ_H 7.61−7.73 (m, 10H, Ph), 7.78 (dd, J_{HH} = 8.3 Hz, J_{HP} = 11.7 Hz, 2H, H^3), 8.17 (d, J_{HH} = 8.3 Hz, 2H, H^2). ^{19}F NMR (d_6-acetone, 376 MHz): δ_F −79.3 (s). $^{31}P\{^1H\}$ NMR (d_6-acetone, 162 MHz): δ_P 45.8 (s). IR (KBr): 3058 ν(O−H), 1719 ν(C═O), 1224, 637 (CF_3SO_3) cm^{-1}.

*Synthesis of [Cr(CO)$_5$(PPh$_2$C$_6$H$_4$CO$_2$H)] (ortho (**9**) and para (**10**)).* To a suspension of [Cr(CO)$_6$] (110 mg, 0.5 mmol) in 30 mL of acetonitrile was added a solution of Me_3NO (35 mg, 0.5 mmol) in 30 mL of acetonitrile. The mixture was stirred for 3 h under inert atmosphere at room temperature. Solvent was removed under vacuum, and the residue was dissolved in tetrahydrofuran (20 mL). Then, a solution of the corresponding diphenylphosphinobenzoic acid (**1** or **2**: 153 mg, 0.5 mmol) in tetrahydrofuran (20 mL) was added dropwise. After stirring for 2 h, the solvent was removed under vacuum. The dry residue was washed with cold pentane and recrystallized from diethyl ether to give **9**−**10** as greenish yellow solids. Yield of **9**: 150 mg, 60%. Mp: 250 (dec.). Anal. Calcd: C, 57.84; H, 3.03; N, 0. Found: C, 58.14; H, 3.42; N, 0. ^1H NMR (d_6-acetone, 400 MHz): δ_H 7.08 (dd, J_{HH} = 8.0 and J_{HP} = 11.8 Hz, 1H, H^3), 7.42−7.71 (m, 12H, H^4 + H^5 + Ph), 8.27 (br, 1H, H^6). $^{31}P\{^1H\}$ NMR (d_6-acetone, 162 MHz): δ_P 61.5 (s). IR (KBr): 2064, 1985, 1931 ν(CO), 1696 ν(C═O) cm^{-1}. Yield of **10**: 112 mg, 45%. Mp: 87. Anal. Calcd: C, 57.84; H, 3.03; N, 0. Found: C, 58.11; H, 3.40; N, 0. ^1H NMR (d_6-acetone, 400 MHz): δ_H 7.56−7.61 (m, 10H, Ph), 7.66 (dd, J_{HH} = 8.3 and J_{HP} = 10.1 Hz, 2H, H^3), 8.17 (dd, J_{HH} = 8.3 and J_{HP} = 1.8 Hz, 2H, H^2). $^{31}P\{^1H\}$ NMR (d_6-acetone, 162 MHz): δ_P 56.2 (s). IR (KBr): 2064, 1989, 1934 ν(CO), 1702 ν(C═O) cm^{-1}.

Reactions to Prepare Hydrogen-Bonded Triazine−Metallo−Organic Acid Adducts, T^n. Supramolecular complexes were prepared from the pure components (triazine, **T**, and the various acids **1**−**10**). Exact stoichiometric molar amounts of the two compounds were dissolved in dry tetrahydrofuran at room temperature, and solvent was swept off by passing a stream of gaseous nitrogen, affording the adducts as pale brown (free phosphines and gold) or green (chromium) waxy solids. The corresponding **T^n** materials where then studied. Only **T^2**, **T^4**, **T^8**, and **T^{10}** were unambiguously identified as hydrogen-bonded adducts.

SingleCrystal Structure Determination of Metallo−Organic Acids 4, 5, 6, and 9. CCDC 1000572−1000575 contain the supplementary crystallographic data for **4**, **5**, **6**, and **9**. These data can be obtained free of charge from the Cambridge Crystallographic Data Centre via www.ccdc.cam.ac.uk/data_request/cif. Crystals of **4** and **9** were obtained by slow diffusion of hexanes into an acetone (**4**) or a dichloromethane (**9**) solution at −18 °C. Crystals of **5** and **6** were obtained by slow diffusion of diethyl ether into chloroform solutions at −18 °C. Crystals were then mounted on a glass fiber and transferred to the SuperNova Oxford Diffraction diffractometer. Crystal data and details of data collection and structure refinement are given in Table 6. Cell parameters, data reduction, and absorption corrections were carried out with the CrysAlis system software.[30] The structure was refined anisotropically on F^2.[31] All non-hydrogen atomic positions were located in difference Fourier maps and refined anisotropically. Hydrogen atoms were placed in their geometrically generated positions. The structure of **4** contains some disordered solvent molecules, and we were unable to properly model it. Compound **5** crystallizes with incipiently disordered diethyl ether and water molecules. Compound **6** crystallizes with an incipiently disordered chloroform molecule. The four molecules of Cr(0) in the unit cell of **9** crystallize with one highly disordered hexane molecule.

■ ASSOCIATED CONTENT

Ⓢ Supporting Information

X-ray crystallographic details in CIF format; FTIR spectra of triazine, chromium metallo−organic acid **10**, and the corresponding aggregate with the triazine **T^{10}**; DOSY spectra of **T^2** and **T^{10}**; polarized optical microscopic texture observed for the free triazine **T** and aggregates **T^2**, **T^4**, **T^8**, and **T^{10}** obtained on cooling from isotropic liquid at room temperature; DSC thermograms for the free triazine **T** and aggregates **T^2**, **T^4**, **T^8**, and **T^{10}**; X-ray diffraction patterns not included in the text; excitation and emission data for all compounds and adducts. This material is available free of charge via the Internet at http://pubs.acs.org.

■ AUTHOR INFORMATION

Corresponding Authors

*E-mail: bardaji@qi.uva.es.
*E-mail: scoco@qi.uva.es.
*E-mail: espinet@qi.uva.es.

Notes

The authors declare no competing financial interest.

■ ACKNOWLEDGMENTS

We thank the Spanish Comisión Interministerial de Ciencia y Tecnología (Project CTQ2011-25137) and the Junta de Castilla y León (Project VA302U13) for financial support. The authors acknowledge SOLEIL for provision of synchrotron radiation facilities, particularly Dr. Javier Pérez for assistance in using beamline SWING. B. H. and B. D. thank the CNRS for support.

■ REFERENCES

(1) (a) Ringsdorf, H.; Schlarb, B.; Venzmer, J. *Angew. Chem., Int. Ed.* **1988**, *27*, 113−158. (b) Zeng, F.; Zimmerman, S. C. *Chem. Rev.* **1997**, *97*, 1681−1712. (c) Kato, T.; Mizoshita, N.; Kishimoto, K. *Angew. Chem., Int. Ed.* **2006**, *45*, 38−68. (d) Lehn, J.-M. *Chem. Soc. Rev.* **2007**, *36*, 151−161. (e) Lehn, J.-M. *Top. Curr. Chem.* **2007**, *322*, 1−32. (f) Rosen, B. M.; Wilson, C. J.; Wilson, D. A.; Peterca, M.; Imam, M. R.; Percec, V. *Chem. Rev.* **2009**, *109*, 6275−6540. (g) Lehn, J. M. *Angew. Chem., Int. Ed.* **2013**, *52*, 2836−2850. (h) Tschierske, C. *Angew. Chem., Int. Ed.* **2013**, *52*, 8828−8878. (i) Rosen, B. M.; Roche, C.; Percec, V. *Top. Curr. Chem.* **2013**, *333*, 213−253.

(2) (a) Kato, T.; Fréchet, J. M. *J. Am. Chem. Soc.* **1989**, *111*, 8533−8534. (b) Brienne, M.-J.; Gabard, J.; Lehn, J.-M.; Stibor, I. *J. Chem. Soc., Chem. Commun.* **1989**, 1868−1870. (c) Willis, K.; Price, D. J.; Adams, H.; Ungar, G.; Bruce, D. W. *J. Mater. Chem.* **1995**, *5*, 2195−2199. (d) Suárez, M.; Lehn, J.-L.; Zimmerman, S. C.; Skoulios, A.; Heinrich, B. *J. Am. Chem. Soc.* **1998**, *120*, 9526−9532. (e) Grunert, M.; Howie, R. A.; Kaeding, A.; Imrie, C. T. *J. Mater. Chem.* **1997**, *7*, 211−214. (f) Würthner, F.; Yao, S.; Heise, B.; Tschierske, C. *Chem. Commun.* **2001**, 2260−2261. (g) Mizoshita, N.; Monobe, H.; Inoue, M.; Ukon, M.; Watanabe, T.; Shimizu, Y.; Hanabusa, K.; Kato, T. *Chem. Commun.* **2002**, 428−429. (h) Jin, S.; Ma, Y.; Zimmerman, S. C.; Cheng, S. Z. D. *Chem. Mater.* **2004**, *16*, 2975−2977. (i) Kajitani, T.; Kohmoto, S.; Yamamoto, M.; Kishikawa, K. *Chem. Mater.* **2004**, *16*, 2329−2331. (j) McCubbin, J. A.; Tong, X.; Zhao, Y.; Snieckus, V.; Lemieux, R. P. *Chem. Mater.* **2005**, *17*, 2574−2581. (k) Barberá, J.; Puig, L.; Romero, P.; Serrano, J. L.; Sierra, T. *J. Am. Chem. Soc.* **2006**, *128*, 4487−4492.

(3) (a) Tschierske, C. *Prog. Polym. Sci.* **1996**, *21*, 775−852. (b) Paleos, C. M.; Tsiourvas, D. *Liq. Cryst.* **2001**, *28*, 1127−1161. (c) Bruce, D. W. *Adv. Inorg. Chem.* **2001**, *52*, 151−204.

(4) (a) Kaafarani, B. R. *Chem. Mater.* **2011**, *23*, 378−396. (b) Pisula, W.; Kastler, M.; Wasserfallen, D.; Mondeshki, M.; Piris, J.; Schnell, I.; Mullen, K. *Chem. Mater.* **2006**, *18*, 3634−3640. (c) O'Neill, M.; Kelly, S. M. *Adv. Mater.* **2003**, *15*, 1135−1146. (d) Kumar, S. *Chem. Soc. Rev.* **2006**, *35*, 83−109. (e) Laschat, S.; Baro, A.; Steinke, N.; Giesselmann, F.; Hagele, C.; Scalia, G.; Judele, R.; Kapatsina, E.; Sauer, S.; Schreivogel, A.; Tosoni, M. *Angew. Chem., Int. Ed.* **2007**, *46*, 4832−4887. (f) Sergeyev, S.; Pisulab, W.; Geerts, Y. H. *Chem. Soc. Rev.* **2007**, *36*, 1902−1929.

(5) Donnio, B.; Guillon, D.; Bruce, D. W.; Deschenaux, R. Metallomesogens. In *Comprehensive Coordination Chemistry II: From Biology to Nanotechnology*; McCleverty, J. A., Meyer, T. J., Eds.;

Elsevier: Oxford, 2003; Vol. 7 (Fujita, M.; Powell, A., Vol. Eds.), Chapter 7.9, pp 357−627.
(6) (a) Deschenaux, R.; Monnet, F.; Serrano, E.; Turpin, F.; Levelut, A.-M. *Helv. Chim. Acta* **1998**, *81*, 2072−2077. (b) Massiot, P.; Imperór-Clerc, M.; Veber, M.; Deschenaux, R. *Chem. Mater.* **2005**, *17*, 1946−1951. (c) Donnio, B.; Seddon, J. M.; Deschenaux, R. *Organometallics* **2000**, *19*, 3077−3081.
(7) Ziessel, R.; Pickaert, G.; Camerel, F.; Donnio, B.; Guillon, D.; Césario, M.; Prange, T. *J. Am. Chem. Soc.* **2004**, *126*, 12403−12413.
(8) Giménez, R.; Elduque, A.; López, J. A.; Barberá, J.; Cavero, E.; Lantero, I.; Oro, L. A.; Serrano, J. L. *Inorg. Chem.* **2006**, *45*, 10363−10370.
(9) (a) Li, S.-Y.; Chen, C.-J.; Lo, P.-Y.; Sheu, H.-S.; Lee, G.-H.; Lai, C. K. *Tetrahedron* **2010**, *66*, 6101−6112. (b) Wang, Y. J.; Song, J. H.; Lin, Y. S.; Lin, C.; Sheu, H. S.; Lee, G. H.; Lai, C. K. *Chem. Commun.* **2006**, 4912−4914.
(10) (a) Coco, S.; Espinet, E.; Espinet, P.; Palape, I. *Dalton Trans.* **2007**, 3267−3272. (b) Coco, S.; Cordovilla, C.; Domínguez, C.; Espinet, P. *Dalton Trans.* **2008**, 6894−6900.
(11) Dechambenoit, P.; Ferlay, S.; Donnio, B.; Guillon, D.; Hosseini, M. W. *Chem. Commun.* **2011**, *47*, 734−736.
(12) (a) Goldmann, D.; Dietel, R.; Janietz, D.; Schmidt, C.; Wendorff, J. H. *Liq. Cryst.* **1998**, *24*, 407−411. (b) Barberá, J.; Puig, L.; Serrano, J. L.; Sierra, T. *Chem. Mater.* **2004**, *16*, 3308−3317. (c) Barberá, J.; Puig, L.; Serrano, J. L.; Sierra, T. *Chem. Mater.* **2005**, *17*, 3763−3771.
(13) Coco, S.; Cordovilla, C.; Domínguez, C.; Donnio, B.; Espinet, P.; Guillon, D. *Chem. Mater.* **2009**, *21*, 3282−3289.
(14) Domínguez, C.; Heinrich, B.; Donnio, B.; Coco, S.; Espinet, P. *Chem.—Eur. J.* **2013**, *19*, 5988−5995.
(15) Chen, H. H.; Lin, H. A.; Chien, S. C.; Wang, T. H.; Hsu, H. F.; Shih, T. L.; Wu, C. *J. Mater. Chem.* **2012**, *22*, 12718−12722.
(16) (a) Schumann, H.; Hemling, H.; Ravindar, V.; Badrieh, Y.; Blum, J. *J. Organomet. Chem.* **1994**, *469*, 213−219. (b) Wong, W.-K.; Zhang, L.; Wong, W.-T. *Chem. Commun.* **1998**, 673−674. (c) Barbaro, P.; Ghilardi, C. A.; Midollini, S.; Orlandini, A.; Ramirez, J. A.; Scapacci, G. *J. Organomet. Chem.* **1998**, *555*, 255−262. (d) Komon, Z. J. A.; Bu, X.; Bazan, G. C. *J. Am. Chem. Soc.* **2000**, *122*, 12379−12380. (e) Correia, J. D. G.; Domingos, A.; Santos, I.; Bolzati, C.; Refosco, F.; Tisato, F. *Inorg. Chim. Acta* **2001**, *315*, 213−219. (f) Kuang, S.-M.; Fanwick, P. E.; Walton, R. A. *Inorg. Chem.* **2002**, *41*, 405−412. (g) Kuang, S.-M.; Fanwick, P. E.; Walton, R. A. *Inorg. Chem. Commun.* **2002**, *5*, 134−138. (h) Kuang, S.-M.; Fanwick, P. E.; Walton, R. A. *Inorg. Chem.* **2002**, *41*, 1036−1038. (i) Kuang, S.-M.; Fanwick, P. E.; Walton, R. A. *Inorg. Chim. Acta* **2002**, *338*, 219−227. (j) Sánchez, G.; García, J.; Meseguer, D.; Serrano, J. L.; García, L.; Pérez, J.; López, G. *Dalton Trans.* **2003**, 4709−4717. (k) Schultz, T.; Pfaltz, A. *Synthesis* **2005**, 1005−1011. (l) Rueff, J.-M.; Perez, O.; Leclaire, A.; Couthon-Gourves, H.; Jaffres, P.-A. *Eur. J. Inorg. Chem.* **2009**, 4870−4876. (m) Phadnis, P. P.; Dey, S.; Jain, V. K.; Nethaji, M.; Butcher, R. J. *Polyhedron* **2006**, *25*, 87−94. (n) Kawatsura, M.; Ata, F.; Wada, S.; Hayase, S.; Uno, H.; Itoh, T. *Chem. Commun.* **2007**, 298−300. (o) Samec, J. S. M.; Grubbs, R. H. *Chem.—Eur. J.* **2008**, *14*, 2686−2692. (p) Uhl, W.; Bock, H. R.; Hepp, A.; Rogel, F.; Voss, M. *Z. Anorg. Allg. Chem.* **2010**, *636*, 1255−1262. (q) Uhl, W.; Bock, H. R.; Kosters, J.; Voss, M. *Z. Anorg. Allg. Chem.* **2010**, *636*, 1851−1859.
(17) Chandrasekaran, A.; Day, R. O.; Holmes, R. R. *Inorg. Chem.* **2001**, *40*, 6229−6238.
(18) Mohr, F.; Jennings, M. C.; Puddephatt, R. J. *Angew. Chem., Int. Ed.* **2004**, *43*, 969−971.
(19) Howe, B. P.; Parish, R. V.; Pritchard, R. G. *Quim. Nova* **1998**, *21*, 564−568.
(20) Pellei, M.; Lobbia, G. G.; Santini, C.; Spagna, R.; Camalli, M.; Fedeli, D.; Falcioni, G. *Dalton Trans.* **2004**, 2822−2828.
(21) (a) Kaharu, T.; Matsubara, H.; Takahashi, S. *J. Mater. Chem.* **1992**, *2*, 43−47. (b) Kaharu, T.; Matsubara, H.; Takahashi, S. *Mol. Cryst. Liq. Cryst.* **1992**, *220*, 191−199. (c) Bruce, D. W.; Lea, M. S.; Marsden, J. R.; Rourke, J. P.; Tajbakhsh, A. R. *J. Mater. Chem.* **1994**, *4*, 1017−1020. (d) Rourke, J. P.; Bruce, D. W.; Marder, T. B. *J. Chem. Soc., Dalton Trans.* **1995**, 317−318. (e) Bruce, D. W.; Lea, M. S.; Marsden, J. R. *Mol. Cryst. Liq. Cryst.* **1996**, *275*, 183−194. (f) Tsiourvas, D.; Kardassi, D.; Paleos, C. M.; Gehant, S.; Skoulios, A. *Liq. Cryst.* **1997**, *23*, 269−274. (g) Barral, M. C.; Jiménez-Aparicio, R.; Priego, J. L.; Royer, E. C.; Torres, M. R.; Urbanos, F. A. *Inorg. Chem. Commun.* **1999**, *2*, 153−155. (h) Tsiourvas, D.; Kardassi, D.; Paleos, C. M.; Skoulios, A. *Liq. Cryst.* **2000**, *27*, 1213−1217. (i) Hatano, T.; Kato, T. *Chem. Commun.* **2006**, 1277−1279. (j) Frein, S.; Auzias, M.; Sondenecker, A.; Vieille-Petit, L.; Guintchin, B.; Maringa, N.; Süss-Fink, G.; Barberá, J.; Deschenaux, R. *Chem. Mater.* **2008**, *20*, 1340−1343. (k) Bottazzi, T.; Cecchi, F.; Zelcer, A.; Heinrich, B.; Donnio, B.; Guillon, D.; Cukiernik, F. D. *J. Coord. Chem.* **2013**, *66*, 3380−3390.
(22) Steiner, T. *Angew. Chem., Int. Ed.* **2002**, *41*, 48−76.
(23) Pitifully the IR spectrum in the range of ν(C═O) and ν(C═N) absorptions does not provide clear-cut information on formation of hydrogen bonds due to low quality of the spectra (arising from the phyical state of the noncrystalline samples) and easy overlap of the carboxylic acid and the triazine bands. This also applies to the group of compounds that are adducts.
(24) For other related nondiscotic mesogens with three-fold symmetry see: (a) Meier, H.; Lehmann, M. *Angew. Chem., Int. Ed.* **1998**, *37*, 643−645. (b) Omenat, A.; Barberá, J.; Serrano, J. L.; Houbrechts, S.; Persoons, A. *Adv. Mater.* **1999**, *11*, 1292−1295. (c) Meier, H.; Lehmann, M.; Kolb, U. *Chem.—Eur. J.* **2000**, *6*, 2462−2469. (d) Lee, C. H.; Yamamoto, T. *Tetrahedron Lett.* **2001**, *42*, 3993−3996. (e) Attias, A.-J.; Cavalli, C.; Donnio, B.; Guillon, D.; Happiot, P.; Malthête, J. *Chem. Mater.* **2002**, *14*, 375−384. (f) Meier, H.; Holst, H. C.; Oehlhof, A. *Eur. J. Org. Chem.* **2003**, 4173−4180. (g) Gómez-Lor, B.; Alonso, B.; Omenat, A.; Serrano, J.-L. *Chem. Commun.* **2006**, 5012−5014. (h) Lehmann, M.; Jahr, M.; Donnio, B.; Graf, R.; Gemming, S.; Popov, I. *Chem.—Eur. J.* **2008**, *14*, 3562−3576. (i) Lehmann, M.; Jahr, M. *Chem. Mater.* **2008**, *20*, 5453−5456. (j) Lehmann, M.; Jahr, M.; Grozema, F. C.; Abellon, R. D.; Siebbeles, L. D. A.; Muller, M. *Adv. Mater.* **2008**, *20*, 4414−4418. (k) Kotha, S.; Kashinath, D.; Kumar, S. *Tetrahedron Lett.* **2008**, *49*, 5419−5423. (l) Lehmann, M. *Chem.—Eur. J.* **2009**, *15*, 3638−3651. (m) García-Frutos, E. M.; Pandey, U. K.; Termine, R.; Omenat, A.; Barberá, J.; Serrano, J. L.; Golemme, A.; Gómez-Lor, B. *Angew. Chem., Int. Ed.* **2011**, *50*, 7399−7402. (n) Achalkumar, A. S.; Hiremath, U. S.; Shankar Rao, D. S.; Krishna Prasad, S.; Yelamaggad, C. V. *J. Org. Chem.* **2013**, *78*, 527−544.
(25) (a) Roundhill, D. M.;. Fackler, J. P., Jr. *Optoelectronic Properties of Inorganic Compounds*; Plenum Press: New York, 1998. (b) Balch, A. L. *Angew. Chem., Int. Ed.* **2009**, *48*, 2641−2644. (c) Tiekink, E. R.T.; Kang, J.-G. *Coord. Chem. Rev.* **2009**, *253*, 1627−1648. (d) He, X.; Yam, V. W. W. *Coord. Chem. Rev.* **2011**, *255*, 2111−2123.
(26) Herbst, A.; Bronner, C.; Dechambenoit, P.; Wenger, O. S. *Organometallics* **2013**, *32*, 1807−1814 and references therein.
(27) Usón, R.; Laguna, A.; Laguna, M. *Inorg. Synth.* **1989**, *26*, 85−91.
(28) Usón, R.; Laguna, A.; Laguna, M.; Fernández, E.; Jones, P. G.; Sheldrick, G. M. *J. Chem. Soc., Dalton Trans.* **1982**, 1971−1976.
(29) Bardají, M.; Crespo, O.; Laguna, A.; Fischer, A. K. *Inorg. Chim. Acta* **2000**, *304/1*, 7−16.
(30) *CrysAlisPro Software system*, Version 1.171.32; Xcalibur CCD system; Oxford Diffraction, Oxford Ltd.: Oxford, 2007.
(31) *SHELXTL program system*, version 5.1; Bruker Analytical X-ray Instruments Inc.: Madison, WI, 1998.